INSTITUTE FOR FUSION STUDIES

DOE/ET-53088-551 IFSR #551

Stochastic Diffusion and Kolmogorov Entropy in Regular and Random Hamiltonians

M.B. ISICHENKO,[a] W. HORTON
Institute for Fusion Studies
The University of Texas at Austin
Austin, Texas 78712
and
D.E. KIM, E.G. HEO, D.-I. CHOI
Korea Advanced Institute of Science and Technology
Seoul, Korea

May 1992

[a] *Also at Kurchatov Institute of Atomic Energy, Moscow, Russia*

THE UNIVERSITY OF TEXAS

AUSTIN

Stochastic Diffusion and Kolmogorov Entropy in Regular and Random Hamiltonians

M.B. Isichenko[a] and W. Horton
Institute for Fusion Studies
The University of Texas at Austin
Austin, Texas 78712, U.S.A.
and
D.E. Kim, E.G. Heo, D.-I. Choi
Korea Advanced Institute of Science and Technology
Seoul, Korea

Abstract

The scalings of the $\mathbf{E} \times \mathbf{B}$ turbulent diffusion coefficient D and the Kolmogorov entropy K with the potential amplitude $\tilde{\phi}$ of the fluctuation are studied using the geometrical analysis of closed and extended particle orbits for several types of drift Hamiltonians. The high-amplitude scalings, $D \propto \tilde{\phi}^2$ or $\tilde{\phi}^0$ and $K \propto \log \tilde{\phi}$, are shown to arise from different forms of a periodic (four-wave) Hamiltonian $\tilde{\phi}(x, y, t)$, thereby explaining the controversy in earlier numerical results. For a quasi-random (six-wave) Hamiltonian numerical data for the diffusion $D \propto \tilde{\phi}^{0.92 \pm 0.04}$ and the Kolmogorov entropy $K \propto \tilde{\phi}^{0.56 \pm 0.17}$ are presented and compared with the percolation theory predictions $D_p \propto \tilde{\phi}^{0.7}$, $K_p \propto \tilde{\phi}^{0.5}$. To study the turbulent diffusion in a general form of Hamiltonian, a new approach of the series expansion of the Lagrangian velocity correlation function is proposed and discussed.

[a] Also at Kurchatov Institute of Atomic Energy, 123182 Moscow, Russia.

I. Introduction

For low-frequency ($\omega \ll \omega_{ce}, \omega_{ci}$) and long wavelength ($k_\perp \rho \ll 1$) fluctuations typically present in plasmas, the motion of the particles are governed by drift equations. As is well known, for broad frequency and amplitude fluctuation spectra, the system easily becomes stochastic exhibiting the sensitive dependence of particle orbits on the initial conditions and a diffusion-like motion of the particles. Less well known is that even for the simplest periodic systems of four plane electrostatic waves (previously referred to as "two-wave systems") the motion also becomes stochastic under easily satisfied conditions.[1–3] In the four-wave regime, however, the numerically measured scaling of the diffusion coefficient on the amplitude of the fluctuation has been in controversy.[2,3] The goal of the present paper is to analytically resolve this controversy by scrutinizing the differences in the previous models,[2–4] as well as to numerically study a new model of stochastic plasma transport associated with a quasi-random (six-wave) Hamiltonian.

As noted by Kleva and Drake,[2] the usual quasilinear theory is inappropriate to the simple systems of several waves with moderate to high amplitude of the fluctuations. Dupree's improvement on the quasilinear theory includes the orbit corrections due to the fluctuations. But the Dupree work does not have the physics necessary to describe the exponential divergence of nearby orbits, because his work is before the advent of modern stochastic theory.

In the present work, we investigate the diffusion coefficient and the stochastic exponentiation in the simplest systems. We study the transport of the guiding centers in a homogeneous constant magnetic field, supporting several transversely propagating, electrostatic, fluctuations. These drift-type waves are easily observed in the tokamak or other fusion devices which have a confining magnetic field and density or temperature gradient.

The previous studies of Kleva and Drake[2] and Horton[3] show significant difference in the

diffusion coefficient with respect to the amplitude of the fluctuations. At high amplitude Horton reports results $D \propto \tilde{\phi}$, and $D \propto \tilde{\phi}^{0.8}$ depending on the value of $\tilde{\phi}$ and the wave phase velocity, whereas Kleva and Drake obtain $D \propto \tilde{\phi}^2$ at high amplitude. Chernikov *et al.*[4] calculate analytically the diffusion varying as $D \propto \tilde{\phi}^0$, for somewhat different Hamiltonians. Here we reconsider these studies in an attempt to find the relationship between these results.

In this work, we use two different analytical approaches to study the large-amplitude behaviors of stochastic diffusion of these systems. The first approach is based on the geometrical analysis of phase-space particle orbits for periodic Hamitonians. In this method, we are able to analytically describe closed and extended orbits that assume distinct roles in the diffusion process. Taking into account these properties leads to the scalings of diffusion, such as $D \propto \tilde{\phi}^2$ and $\tilde{\phi}^0$, while the Kolmogorov entropy is found to behave logarithmically, $K \propto \log \tilde{\phi}$. These results are consistent with the earlier numerical calculations of Kleva and Drake[2] and Horton[3].

The second approach employs the two-time particle velocity correlation function, which is shown to be in principle calculable, for any specified Hamiltonian, in the form of an asymptotic series. As is well known, the time integral of the velocity correlation function is the diffusion coefficient. We regroup the terms of the series to heuristically predict the diffusion scaling $D \propto \tilde{\phi}^0$. However, this method suffers drawbacks due to the apparently conditional convergence of the correlation function series. We also provide numerical results on the velocity correlation function.

For a random, nonperiodic, short-range correlated potential, the percolation theory[5,6] predicts $D \propto \tilde{\phi}^{7/10}$, $K \propto \tilde{\phi}^{1/2}$. We attempt to numerically prove these results by introducing the model of a quasiperiodic (six-wave) Hamiltonian. However, our numerical results $D \propto \tilde{\phi}^{0.92\pm0.04}$ and $K \propto \tilde{\phi}^{0.56\pm0.17}$ show only partial agreement with the theory, and we point out the reasons likely responsible for the discrepancy.

The work is organized as follows. In Sec. II we introduce the fluctuating electrostatic

potential given in Refs. 2 and 3 and the stream function of Ref. 4, which take the status of the Hamiltonian of the problem giving the perpendicular equation of t ıe motion. Here we give a geometric i analysis of phase-space orbits in Kleva-Drake[2], Horton[3], and Chernikov *et al.*[4] Hamiltonians, which casts a light on the origin of different scalings of the stochastic diffuson. In Sec. III we consider the stochastic exponentiation of nearby particle orbits and derive the logarithmic scaling of the Kolmogorov entropy in spatially periodic flows. In Sec. IV we present a computer study of diffusion and Kolmogorov entropy in a six-wave (quasi-random) Hamiltonian. I Sec. V we relate the velocity correlation function with the diffusion coefficient and ana.yze, both ı alytically and numerically, the scaling of the correlation time and the diffusion. In Sec. \ I the res.its are briefly summarized and discussed.

II. Particle orbits and diffusion scalings in periodic potentials

A. Equations of motion

We assume that there exists a uniform magnetic field along the z direction i.e., $\mathbf{B} = B\hat{\mathbf{z}}$, where $\hat{\mathbf{z}}$ is the unit vector along the z direction. Suppose that there are electrostatic waves propagating perpendicularly to the magnetic field. If such waves have a long wavelength ($k_\perp \rho \ll 1$) and a low frequency ($\omega/\omega_c \ll 1$), the motion of the particles can be described by drift equation. That is, the particle motion is given by the $\mathbf{E} \times \mathbf{B}$ velocity

$$\mathbf{v}(\mathbf{x}, t) = c\frac{\mathbf{E} \times \mathbf{B}}{B^2} = c\frac{\hat{\mathbf{z}} \times \nabla\Phi}{B} \tag{1}$$

where Φ is the electrostatic potential. In general, $\Phi = \overline{\Phi}(\mathbf{x}) + \tilde{\Phi}(\mathbf{x}, t)$. In component form the equations of the two-dimensional particle motion become

$$\frac{dx}{dt} = -\frac{\partial}{\partial y}\left(\frac{c}{B}\Phi(x, y, t)\right) \tag{2}$$

$$\frac{dy}{dt} = \frac{\partial}{\partial x}\left(\frac{c}{B}\,\Phi(x,y,t)\right) \ . \tag{3}$$

Thus our system is a Hamiltonian system with canonical momentum and coordinate $(p,q) = (x,y)$ and with the time-dependent Hamiltonian $H = (c/B)\,\Phi(x,y,t)$. This corresponds to a 3/2-degrees-of-freedom Hamiltonian motion, which is typically chaotic.

In the present work we consider several Hamiltonians in the form of N travelling waves,

$$H(x,y,t) = \sum_{i=1}^{N} A_i \sin(\mathbf{k}_i\mathbf{x} - \omega_i t + \theta_i) \ , \tag{4}$$

which may be viewed as a truncated form of a general Fourier series expansion. Henceforth, we refer to expression (4), or its standing-wave analogue with $\omega_i = 0$ and $A_i = A_i(t)$, as the N-wave Hamiltonian. For case of $N \leq 2$, the system is integrable because it is possible (except for special cases) to change the coordinate system to that where the potential is time-independent. For multiple waves having the same vector phase velocity, the situation is the same. The integrable cases are studied by Horton.[1,3] Here we focus on the case of nonintegrable, chaotic motion.

B. Invariance scaling

For the N-wave system with $N \geq 3$, the motion from Eqs. (2)–(4) is (almost) always stochastic diffusion.[1–3] The space-time scale of the stochastic diffusion can be determined from the space-time scale $(1/k, 1/\omega)$ and the amplitude Φ of $\Phi(\mathbf{x},t)$ due to the invariance scaling. With $\mathbf{x} = (x,y)$, Eqs. (2) and (3) are invariant to the transformation $k\mathbf{x} \rightarrow \mathbf{x}'$ and $ck^2\,\Phi t/B \rightarrow t' = \Omega_E t'$ where Ω_E^{-1} is the characteristic time to rotate around the potential structure of scale $1/k$.

This transformation $(\mathbf{x},t) \rightarrow (\mathbf{x}',t')$ takes $d\mathbf{x}/dt = (k\Phi/B)\mathbf{F}(k\mathbf{x},\omega t)$ to the form $d\mathbf{x}'/dt' = \mathbf{F}(\mathbf{x}',\omega t'/\Omega_E)$ with the diffusion in $\mathbf{x}', t'$ space given by $D_{\mathbf{x}'} = \widehat{D}(\omega/\Omega_E)$. Transforming back to $(\mathbf{x},t)$ variables the diffusion is found to be of the form

$$D = \frac{c\Phi}{B}\,\widehat{D}\left(\frac{\omega B}{ck^2\,\Phi}\right) \ . \tag{5}$$

In earlier work,[3,6] the nondimensional wave amplitude $R_E = ck^2\Phi/B|\omega|$ is defined with the meaning of the number of rotations round the potential minimum or maximum in a wave period. If $\widehat{D}(z)$ is analytic at $z = 0$ then we would expect $D = (c\Phi/B)[D_0 + D_1(\omega B/ck^2\,\Phi) + D_2(\omega B/ck^2\,\Phi)^2 + \cdots]$. However, the limit D_0 corresponds to $\omega \to 0$, where the system (2)–(3) is integrable, so that the D_1 term is the first surviving dependence of $\widehat{D}(z)$ at small z. For large z the expansion $\widehat{D}(z) \simeq D_{-1}/z$ gives the quasilinear scaling $D_{ql} = (ck\Phi/B)^2\omega^{-1}$ which only applies for $\Omega_E \ll \omega$. Due to the singular nature of the boundary layer between the positive and negative cells, however, the function $\widehat{D}(z)$ may not be analytic at the origin. In fact, Ref. 5 uses percolation theory to argue that, for a random Hamiltonian, $\widehat{D}(z) \simeq z^{3/10}$ for small z. A numerical attempt to find this percolational scaling is reported in Sec. IV.

C. Orbits and diffusion

In this section we present a qualitative theory of stochastic diffusion for several Hamiltonians that were previously studied numerically[2,3] or theoretically[4] and explain the origin of the difference in the previous results.

If we normalize the length and time appropriately, we can take the stochastic Horton[3] Hamiltonian as follows,

$$H^H = \tilde{\phi}[\sin x \cos y + \varepsilon \cos(kx)\cos(qy - \omega t)]\ , \tag{6}$$

which, in the notation of Eq. (4), corresponds to the four-wave Hamiltonian with $k_{1,2} = (1, \pm 1)$, $k_{3,4} = (\pm k, q)$, $\omega_{1,2} = 0$, $\omega_{3,4} = \omega$, $\theta_{1,2} = 0$, $\theta_{3,4} = \pi/2$, and the same wave amplitudes $A_i = \tilde{\phi}/2$. For $k = \varepsilon = 1$ and $q = \omega = 2$, the diffusion in this Hamiltonian was computed[3] to behave as $D \propto \tilde{\phi}^2$ at small $\tilde{\phi}$ and $D \propto \tilde{\phi}^{0.8}$ at $\tilde{\phi} \gg 1$.

The Kleva-Drake[2] Hamiltonian looks very similar to (6),

$$H^{KD} = \tilde{\phi}[(1/k)\cos kx \cos ky + \varepsilon \sin x \cos(y - t)]\ ; \tag{7}$$

however, for $\varepsilon = 1$ and the large amplitude $\tilde{\phi}$ they report a drastically different scalinf $D(k=1) \propto \tilde{\phi}^2$, whereas $D(k=2) \propto \tilde{\phi}^{1/2}$.

Chernikov *et al.*[4] studied a similar problem of passive time-dependent convection that corresponds to the Hamiltonian

$$H^{CNRY} = \tilde{\phi}(\sin x \sin y + \varepsilon y \cos t) \ , \tag{8}$$

and reported the saturating large-amplitude diffusion asymptotics

$$D_{xx} = 2\varepsilon \tag{9}$$

that was found analytically. Hamiltonian (8) is not space-periodic but its velocity field $\mathbf{v} = \hat{\mathbf{z}} \times \boldsymbol{\nabla} H^{CNRY}$ is periodic.

In order to understand the difference between the apparantly similar Hamiltonians (6)–(8), we examine their phase-space portraits (Fig. 1). In Fig. 1(a) the contours of Hamiltonian (6) with $q = 2$ and $\varepsilon \ll 1$ are depicted. Due to periodicity, it is quite possible to plot the potential contours at finite ε; however, it is more convenient to start with the case $\varepsilon \ll 1$. To zeroth approximation ($\varepsilon = 0$), the phase portrait of the Hamiltonian (6) represents a periodic system of square convection cells with all the orbits closed within the cells. The small perturbation, given by the second term on the right-hand side of Eq. (6), preserves the topology of most contours except for those that are close to the separatrices. These contours lie near the zero level of $H(x, y, t)$ and are the primary candidates to produce extended (open) particle orbits.[5] The geometry of these strongly perturbed orbits, whose area fraction is of order ε, is governed by solely the sign of the perturbation in the nodes of the non-perturbed separatrix lattice. Given the commensurability of the periods of the background and of the perturbation, this results in a spatially periodic pattern shown in Fig. 1(a). As the perturbation given by the second term in H^H travels over the unperturbed background, the topology is periodically changing. This process is accompanied by the particle crossover

between closed and extended orbits. Since the direction of the particle displacement on an open orbit depends on the random phase difference between the particle closed-orbit rotation and the perturbation, the process gives rise to diffusion. (A similar transport model was discussed in Ref. 7 for the case of travelling "breathing vortices".) In Fig. 1(a) we see that the open contours of Hamiltonian (6) are localized in the x direction and extended in the y direction.

In the low-amplitude limit, $\tilde{\phi} \ll 1$, the phase of the perturbation changes much faster than the particle passes the distance $k^{-1} \simeq 1$, hence the long-range topography of the potential is irrelevant. The simple, heuristic estimate of the diffusion is then $D \simeq v^2/\omega = \tilde{\phi}^2$ (for $\varepsilon \simeq 1$). This quasilinear result, which should be valid for an ∞-wave Hamiltonian with random phases,[8] was numerically found[3] to also hold for Hamiltonian (6), although in principle, due to the possibly complicated result of the high-frequency averaging, an effective potential with nontrivial diffusion regimes can occur.[4]

In the large-amplitude limit $\tilde{\phi} \gg 1$, which is the subject of our main interest, we have the x displacement of the order of $k^{-1} \simeq 1$ in time $\omega^{-1} \simeq 1$ and the fraction ε of diffusing particles, hence

$$D_{xx} \simeq \varepsilon \ , \quad \tilde{\phi} \gg 1 \ . \tag{10}$$

Eq. (10) is the diffusion in the x direction. Due to the openness of the orbits in the y direction, the particle displacement $\Delta y \simeq v/\omega \simeq \tilde{\phi}$ is much greater than the that in the x direction, assuming the y-diffusion $D_{yy} \simeq \varepsilon\tilde{\phi}^2$.

If the perturbation is extremely small, $\varepsilon \ll 1$, one should take into account the logarithmic correction to the velocity on an open orbit. Due to the logarithmic divergence of the passing time near a saddle, the average velocity on an open orbit is somewhat decreased, $v_\varepsilon \simeq v/|\log\varepsilon|$, leading to the somewhat lower diffusion coefficient $D_{yy} \simeq \varepsilon\tilde{\phi}^2/\log^2\varepsilon$.

The above arguments suggest that for $\tilde{\phi} \gg 1$ and $\varepsilon \ll 1$ all particles can be divided into two distinct groups. The first group includes diffusing particles i.e., those lying close

enough to the separatrices and undergoing the periodic crossover between localized and extended orbits. The second group includes trapped particles, whose closed orbits do not reach the breathing separatrices, and hence remain trapped exponentially long due to the well conserved adiabatic invariant (the area within a closed orbit). However, in the limit of $\varepsilon \simeq 1$ (the "deep breathing" of separatrices) there may be no trapping at all.

Estimate (10) suggests an asymptotic saturation of the diffusion D_{xx} in the Horton model also in the limit $\varepsilon = 1$, which is the marginally applicable case of the above qualitative theory. The slow-down of the diffusion $D_{xx}(\tilde{\phi})$ build-up reported in Ref. 3 may be in fact the transition to this saturation.

The phase portrait of the Kleva-Drake ($k = 1$) model (7) [shown in Fig. 1(b)] is qualitatively different from that of the Horton Hamiltonian [Fig. 1(a)], because some contours of the Kleva-Drake ($k = 1$) Hamiltonian are extended in both the x and the y directions. In the quasilinear limit $\tilde{\phi} \ll 1$, this topology apparently makes no difference in terms of diffusion ($D \propto \tilde{\phi}^2$). However, in the strong turbulence limit $\tilde{\phi} \gg 1$, the particles lying on the extended orbits (with number fraction ε) are carried to a large distance $\Delta x \simeq v_\varepsilon/\omega \simeq \tilde{\phi}/|\log \varepsilon| \gg k^{-1}$ before the phase of the perturbation is changed. Fig. 1(b) shows that the diffusing particles periodically undertake long "North-East" (or, with the same probability, "South-West") flights during the first half perturbation period. During the second half period, the flights become SE or NW. This clearly leads to the approximately isotropic diffusion with the coefficient

$$D_{xx} \simeq D_{yy} \simeq \varepsilon(\Delta x)^2 \omega \simeq \frac{\varepsilon}{\log^2 \varepsilon}\,\tilde{\phi}^2 \ , \quad \tilde{\phi} \gg 1, \quad \varepsilon \ll 1 \ . \tag{11}$$

This quadratic behavior of stochastic diffusion was reported by Kleva and Drake[2], who also explicitly computed the SW-NE-SE-NW-like flights, although for $\varepsilon = 1$. The quadratic dependence (11) is due to the exact periodicity of Hamiltonian (7) tha leads to the averagely straight phase space orbits. In the case of incommensurate wavelengths, $k \neq m/n$, the potential is no longer periodic and one can expect fractal orbits with a slower growth of

$D(\tilde{\phi})$, which can be in general a fractional power function[6,5] of $\tilde{\phi}$. The golden mean $\mu = (\sqrt{5}-1)/2$, which is "the most irrational" number (according to the slowest convergence of its continued fraction representation), was used in Ref. 2 and a significant decrease in diffusion was observed at $k = 1+\mu$ and $3-\mu$, compared to the case $k = 1$. Unfortunately, no scalings for $D(\tilde{\phi})$ were reported for irrational k's. We provide such scalings in Sec. IV.

For the Kleva-Drake Hamiltonian with $k = 2$ [Fig. 1(c)], we notice that the phase space orbits are closed in all directions which implies the same saturating, and isotropic, diffusion as in Eq. (10). The square-root dependence[2] $D \propto \tilde{\phi}^{0.5}$ is likely to be transient towards this saturation. The explanation of the measured logarithmic behavior of the Kolmogorov entropy is presented in Sec. IV.

The apparently similar diffusion saturation of Eq. (9) for Chernikov *et al.* Hamiltonian (8) stems, however, from a different motion pattern. The peculiarity of Hamiltonian (8) is that all its extended streamlines have the same (say, East) direction during one half a period [Fig. 1(d)]. Hence, almost regardless of the initial condition, a diffusing particle makes a fixed long flight in the x direction, $\Delta x \simeq v/\omega \gg k^{-1}$, during its extended-orbit phase. To first approximation, the particle is then trapped to a closed orbit, which has the same adiabatic invariant as that before the flight. On the second half period, the direction of all flights is changed to an opposite (West) and the particle returnes back to its original convection cell. However, due to the random phase of particle rotation at the moment of trapping or release, the particle enters/exits an extended-orbit channel at a random point within one convection cell. Thus the particle return may probabalistically happen to the original cell, as well as to one of its nearest neighbors, hardly farther. This leads to the saturating diffusion behavior as in formula (9). Of course, there would be no stochastic diffusion in the system, were an additional integral of motion (the adiabatic invariant) exactly conserved. In fact, the adiabatic invariant change for passing particles is not exponentially small, due to the mentioned randomness in the particle rotation phase during the separatrix crossing.[9] To

accurately evaluate the numerical constant in expression (9), the change in the adiabatic invariant must be calculated, as demonstrated by Chernikov *et al.*[4]. Another example of saturated stochastic diffusion for the Hamiltonian[4]

$$H = \tilde{\phi}(\sin x \sin t + \cos x \cos t)$$

is of quite the same nature.

III. Kolmogorov entropy

The Kolmogorov entropy serves as a measure of stochastic exponentiation and is usually defined as

$$K = \lim_{t\to\infty} \lim_{d_{12}(0)\to 0} \frac{1}{t} \log \frac{\langle d_{12}(t)\rangle}{d_{12}(0)} , \qquad (12)$$

where $d_{12}(t) = |\mathbf{x}_1(t) - \mathbf{x}_2(t)|$ designates the distance between two neighboring particles following their orbits, and the average over the initial condition $\mathbf{x}_1(0)$ is taken. Without this average formula (12) would define [for almost all orientations of the vector $\mathbf{d}(0)$] the largest Lyapunov exponent $\Lambda_1(\mathbf{x}_1) > 0$, which is a function of the initial point. In a dissipative system, the Lyapunov exponent is constant in the basin of attraction of a chaotic attractor. In a Hamiltonian system, Λ_1 can be an intricate function of $\mathbf{x}_1$. The Komogorov entropy (12) appears to be merely the maximum value of $\Lambda_1(\mathbf{x}_1)$ over the considered region of initial conditions, because in the average of $\langle d_{12}(t)\rangle$ the fastest growing exponent should ultimately dominate the terms with slower exponentiation.

We are not aware of any analytical methods of the direct calculation of quantity (12) for non-quasilinear chaotic flows. Instead, we use the method first proposed by Gruzinov *et al.*,[5] where the set of infinitesimally close particle pairs is replaced by a continuous curve advected by the phase-space flow (2)–(3). The stretching rate of the "liquid curve" is also a natural measure of stochasticity; it can be shown[10] that the growth rate $K = \lim_{t\to\infty} d \log L(t)/dt$

[where $L(t)$ is the appropriately averaged curve length] is the same as the K in expression (12).

Consider, for example, the Kleva-Drake ($k = 1$) Hamiltonian (4) shown in Fig. 1(b). The dominant feature of the liquid curve behavior is that the curve drapes over the saddle points of the flow and gets stretched in the extended channels lying between the separatrices (i.e., the streamlines coming through the saddles). The stretching process is schematically shown in Fig. 2. During the first half period of the perturbation, $\tau = \pi/\omega$, the curve length is stretched approximately $kv_\varepsilon/\omega = \tilde{\phi}/|\log\varepsilon| \gg 1$ times leading to a "fish bone" structure [Fig. 2(a)]. During the second half period, when the direction of the open channels is changed by 90^0, each piece of the primary fish bone is stretched into a "secondary fish bone," so that the liquid curve pattern becomes quite intricate [Fig. 2(b)]. The process will continue, thereby leading to an exponential growth in the curve length,

$$L(t) \simeq L(0)\left(\frac{kv_\varepsilon}{\omega}\right)^{t/\tau} \simeq L(0)\exp(Kt)\ , \tag{13}$$

where the expression

$$K \simeq \tau^{-1}\log\left(\frac{kv_\varepsilon}{\omega}\right) \simeq \tau^{-1}\log\left(\frac{\tilde{\phi}}{|\log\varepsilon|}\right)\ , \quad \tilde{\phi} \gg 1\ , \quad \varepsilon \ll 1\ , \tag{14}$$

yields the desired scaling of the Kolmogorov entropy. Notice that the symbol "$\simeq$" refers only to the expression under logarithm; the prelogarithmic factor τ^{-1}, understood as the reciprocal period of the contour topology change, is exact.

In the above argument we have omitted the discussion of the pieces of the curve lying outside the channels — that is, in the cells of unchanged topology of the streamlines. Obviously, those regions will contribute only linearly growing terms in the curve length $L(t)$ that will become altogether negligible in comparison with the exponentiating part (13).

It is easy to see that the above result (14) holds for all periodic flows shown in Fig. 1 because the openness of the channels is of no special importance for the considered process

of the curve stretching, provided that the topology change (separatrix reconnection) occurs after each period of the perturbation.

The logarithmic dependence $K(\tilde{\phi})$ is consistent with the numerical findings of Kleva and Drake.[2] For the Hamiltonian (7) with $k = 2$, the topology changes occur each time $\tau = \pi/k = \pi/2$. Hence the Kolmogorov entropy should scale as $K = (2/\pi)\log(C\tilde{\phi})$ for $\tilde{\phi} \gg 1$. Kleva and Drake report the Lyapunov exponent $\Lambda_1 = 0.14 \log \tilde{\phi} + 0.33$ for the initial point $\mathbf{x}_1 = (-1.18950, 1.22560)$ that corresponds to approximately one-quarter the maximum Lyapunov exponent given by K. One can imagine that there are regions in the phase plane sufficiently far from the unperturbed separatrices, where the topology change happens rarer, only once a perturbation period $\tau = 2\pi$, which corresponds to the Λ_1 scaling as $(2\pi)^{-1} \log(C\tilde{\phi})$. The initial point taken by Kleva and Drake seems to belong to this category.

Interestingly, the dependence of the Kolmogorov entropy K on the perturbation strength $\varepsilon \ll 1$ is very weak (only doubly-logarithmic), because the narrow widths of the reconnecting channels by no means prevent the fast stretching and folding of a liquid curve.

It is emphasized that behavior (14) is typical for only spatially periodic Hamiltonians or for those possessing only a finite number of saddle points. In a disordered, nonlocalized Hamiltonian, the saddle points can be distributed continuously over the energy level leading to much faster contour reconnection rate (a reconnection occurs when two saddles cross the same energy level) and hence to a different scaling of the Kolmogorov entropy,[5]

$$K \propto \tilde{\phi}^{1/2} \log \tilde{\phi} \,. \tag{15}$$

In the next section we find that this square-root scaling of the Kolmogorov entropy is indeed observed in a generic $\mathbf{E} \times \mathbf{B}$ drift Hamiltonian.

IV. Diffusion in a six-wave Hamiltonian

In order to go beyond the degenerate models of periodic four-wave Hamiltonians, we study numerically the stochastic diffusion and exponentiation in a quasi-random Hamiltonian

$$H(x,y,t) = \tilde{\phi} \sum_{i=1}^{6} \sin(\omega_i t + \phi_i) \sin(\mathbf{k}_i \cdot \mathbf{x} + \theta_i) \ . \tag{16}$$

To introduce randomness, we choose the directions α_i of the wavevectors $\mathbf{k}_i = (k_i \cos\alpha_i, k_i \sin\alpha_i)$, as well as the phases ϕ_i and θ_i, at random and uniformly distributed in $[0, 2\pi]$. After the random numbers are drawn, their values are fixed for all simulations. All amplitudes are taken the same, $A_i \equiv \tilde{\phi}$. To avoid the periodicity in time, the frequencies of the waves are set incommensurate, but of the same order, $\omega_i = (1 + i/5)^{1/2}$. We notice that the absence of the time-periodicity makes the KAM theory not directly applicable, which in turn implies the absence of invariant tori and an unconstrained chaotic transport. Similarly, the wavenumbers $k_i = \omega_i$ are taken to model a linear wave-dispersion relation. The potential contours of (16) are shown in Fig. 3.

We measure the diffusion coefficient solving the equations of motion (2)–(3) and using the usual rule

$$D(t) = \frac{1}{2t} \frac{1}{N_p} \sum_{i=1}^{N_p} [x_i(t) - x_i(0)]^2 \ , \tag{17}$$

where N_p is the number of particles. Like in earlier studies[2,3], the turbulent diffusivity D is determined as the late time average from the time series of $D(t)$,

$$D = \frac{1}{T_{\max} - T_0} \int_{T_0}^{T_{\max}} D(t) dt \ , \tag{18}$$

with the standard deviation

$$\delta D = \left[\frac{1}{T_{\max} - T_0} \int_{T_0}^{T_{\max}} [D(t) - D]^2 dt \right]^{1/2} \ , \tag{19}$$

where T_0 is the time when convergence is visually observed.

The variation of D is shown in Fig. 4 in the amplitude range $1 \leq \tilde{\phi} \leq 120$. The observed dependence, $D \propto \tilde{\phi}^{0.92\pm0.04}$, is appreciably steeper than the one predicted by percolation theory,[6,5] $D \propto \tilde{\phi}^{7/10}$. The discrepancy may be due to the presence of long-range spatial correlations in the Hamiltonian (the correlator $C_H(\mathbf{x}) = \langle H(\mathbf{x}'+\mathbf{x},t)H(\mathbf{x}',t)\rangle_{\mathbf{x}'}$ does not vanish at $|\mathbf{x}| \to \infty$) that may affect the geometry of isopotential contours (the particle orbits at $\tilde{\phi} \gg 1$). Indeed, for a three-wave potential (the lowest number of waves without spatial periodicity), these correlations result in essentially straight open streamlines.[11] So the presence of the correlations, due to the finite number N of waves, tends to result in more extended isopotentials and hence a steeper $D(\tilde{\phi})$ dependence, as compared to the short-range-correlated random flow. Another reference point is given by Ottaviani[12] who has computed the diffusion scaling $D \propto \tilde{\phi}^{0.80\pm0.04}$, which is closer to the percolation-theory prediction, for $N = 64$ standing waves and somewhat different time-dependence. One may expect that the percolational "7/10" scaling becomes asymptotically valid for an infinite number of waves, when the long correlations are irrelevant due to a sufficiently fast fall-off of the wavenumber spectrum at $k \to 0$. This kind of spectrum is referred to as "monoscale."[10]

In addition to diffusion, we compute the Kolmogorov entropy using the definition (12) in a straightforward manner. We average the interparticle separation $d_{12}(t)$ over one hundred pairs of particles, with the initial points distributed randomly in the $(-10\pi,\ 10\pi)^2$ square and the fixed initial separation of $d_{12}(0) = 10^{-4}$. The Kolmogorov entropy K is then calculated as the average slope of $\log d_{12}(t)$ versus time, until $d_{12}(t)$ reaches unity. The dependence of $d_{12}(t)$ (Fig. 5) shows a high degree of intermittency, especially at large $\tilde{\phi}$: most of pairs exhibit a poor separation for a sufficiently long time, and then suddenly diverge to a distance of order unity upon encountering a saddle point of the flow. On the average, however, this divergence of neighboring trajectories is well described in terms of an exponential separation.

The amplitude-dependence of the Kolmogorov entropy (Fig. 4) is approximated by the power law, $K \propto \tilde{\phi}^{0.56\pm0.17}$. Thus we find that, unlike the scaling of diffusion, the computed

Kolmogorov entropy is consistent with the theoretical prediction (15). We ascribe this observation to the fact that the scaling (15) is based[5] on fairly rough properties of the random velocity field and is insensitive to the the presence of long-range correlations in the stream function $H(x, y, t)$.

V. Velocity correlation function

In this section, we try the approach of the Lagrangian velocity correlation function that seems to promise the possibility of the analytical calculation of diffusion for a general Hamiltonian.

A. Theory

When local stochasticity is set up, the behavior of the system of test particles can be described by the diffusion process. The basic assumption for the diffusion approximation is that the particles experience a short correlation time along its trajectory. This correlation time is typically given by the reciprocal Kolmogorov entropy K. The definition of the diffusion coefficient follows from the formal integration of the equation of motion

$$x(t) - x(0) = \int_0^t v_E\left(x(t_1), y(t_1), t_1\right)\, dt_1 \tag{20}$$

where v_E is shorthand for $-\partial H/\partial y = \dot{x}$. Introducing the average $\langle \ldots \rangle$ over the initial conditions $(x(0), y(0))$ in the phase space, the relation

$$\left\langle (x(t) - x(0))^2 \right\rangle = \lim_{t\to\infty} \int_0^t dt_1 \int_0^t dt_2 \left\langle v_E(t_1) v_E(t_2) \right\rangle \simeq 2Dt\ , \qquad \text{as} \qquad t \to \infty\ , \tag{21}$$

defines the diffusion coefficient.

Thus, we are led to study the nature of the two-time velocity correlation function,

$$C(\tau) = \left\langle v_E(t) v_E(t+\tau) \right\rangle\ , \tag{22}$$

where we assume that the average over the initial conditions is time translationally invariant, thus eliminating the t dependence of the velocity correlation function. The definition for D

can be developed further using the time translational invariance of the average to give

$$D = \lim_{t\to\infty} \frac{1}{2t} \int_0^t dt_1 \int_0^t dt_2\, C(t_1 - t_2) = \int_0^\infty d\tau\, C(\tau)\ , \tag{23}$$

where we changed the integration variables from (t_1, t_2) to (τ, ξ), where $\tau = t_1 - t_2$ and $\xi = t_2$. That is, the diffusion coefficient is the time integral of the velocity correlation function, which is a well established result.[13]

It should be noted that because our approach is not a self-consistent turbulence theory — that is, we start from the given waves — the velocity correlation function must be known in principle. Since the system is not integrable, however, we cannot evaluate the correlation function exactly. But we do know the derivatives to any order at $t = 0$, although the algebra becomes extremely complex as the order of the derivatives becomes large. For illustration, we compute

$$C(0) = \langle v_E(0)\, v_E(0) \rangle \tag{24}$$

and

$$\frac{dC(\tau)}{d\tau} = \left\langle v_E(0) \left([v_E(\tau), H] + \frac{\partial v_E(\tau)}{\partial \tau} \right) \right\rangle \tag{25}$$

where $[f, g]$ is the Poisson bracket defined by

$$[f, g] \equiv \frac{\partial f}{\partial y}\frac{\partial g}{\partial x} - \frac{\partial g}{\partial y}\frac{\partial f}{\partial x}\ . \tag{26}$$

Thus we can evaluate $dC(\tau)/d\tau|_{\tau=0}$ explicitly. Recursively, we can compute the higher derivatives

$$\frac{d^{n+1}C(\tau)}{d\tau^{n+1}} = \left\langle v_E(0) \mathcal{D}^{n+1} v_E(\tau) \right\rangle \tag{27}$$

where

$$\mathcal{D}^{n+1} v_E(\tau) = [\mathcal{D}^n v_E(\tau), H] + \frac{\partial}{\partial \tau}\, \mathcal{D}^n v_E(\tau) \quad \text{and} \quad \mathcal{D}^0 v_E(\tau) = v_E(\tau)\ .$$

From these derivatives of the velocity correlation function at $\tau = 0$, we can form a Taylor series expansion about $\tau = 0$:

$$C(\tau) = \sum_{n=0}^{\infty} \frac{\tau^n}{n!} \frac{d^n C(\tau)}{d\tau^n}\bigg|_{\tau=0} . \tag{28}$$

Although this expansion is useless for the evaluation of diffusion coefficient, since the series is not in a closed form, we may hope to infer the time scale of the correlation function as $\tilde{\phi}$ varies. We explicitly computed the first few low order derivatives with help of the symbolic manipulator MACSYMA for the Horton Hamiltonian (6) with $\varepsilon = 1$. The result is

$$C(\tau) = \tilde{\phi}^2 \left(\frac{5}{4} - \frac{95\tilde{\phi}^2 + 128}{64} \tau^2 + \frac{9391\tilde{\phi}^4 + 27072\tilde{\phi}^2 + 8192}{24 \cdot 512} \tau^4 + \cdots \right) . \tag{29}$$

We note that for the $\tilde{\phi} \ll 1$ limit, the time scale is independent of $\tilde{\phi}$, but that for the $\tilde{\phi} \gg 1$ limit, the dependence is on $(\tilde{\phi}\tau)^n$ and thus $\tau_c \simeq 1/\tilde{\phi}$, where the correlation time τ_c is the characteristic time scale of $C(\tau)$.

We consider this approach more systematically. First, it is noted that the derivatives in Eq. (25) consist of two terms, the contribution from $\mathbf{E} \times \mathbf{B}$ convection and from the explicit time dependence of the drift velocity. It is noted that the convective contribution is $\mathcal{O}(\tilde{\phi}^3)$ and the contribution from the explicit time dependence is $\mathcal{O}(\tilde{\phi}^2)$ in Eq. (25). For low fluctuation amplitude $\tilde{\phi} \ll 1$, we may keep only the contribution from the explicit time dependence. In this case we can calculate the derivatives exactly to the infinite order. Then the Taylor series reduces to

$$C(\tau) = \tilde{\phi}^2 \left(\frac{1}{4} + \cos(2\tau) \right) . \tag{30}$$

In this limit, the correlation function is simply sinusoidal oscillations with period π, which is just the period of the driving Hamiltonian. Also we can see that as $\tilde{\phi} \to 0$, the Taylor expansion of Eq. (29) agrees with the expansion of Eq. (30) confirming our calculations. From Eqs. (23) and (30) we note that the quasilinear scaling $D \propto \tilde{\phi}^2$ is far from a self-evident result, and in order to obtain diffusion in a this system one has to account for space

dependence of the Hamiltonian, i.e. to keep Lagrangian derivatives in Eq. (28). In the space-uniform velocity field approximation, a time decaying correlation function $C(\tau)$ can result only from an infinite number of waves with random phases, as actually assumed in the quasilinear theory.[8]

For the other extreme, where $\tilde{\phi} \gg 1$, we keep the contribution from the highest order terms. In this case it is immediately seen that C_n ($\equiv d^n C(\tau)/d\tau^n|_{\tau=0}$) has the leading term proportional to $\tilde{\phi}^{n+2}$ from the convective derivative. Thus we may write

$$C_n \simeq C(0)\left(a_n^n \tilde{\phi}^n + a_{n-1}^n \tilde{\phi}^{n-1} + a_{n-2}^n \tilde{\phi}^{n-2}\right) \tag{31}$$

and

$$C(\tau) = \sum_{n=0}^{\infty} \frac{1}{n!} C_n \tau^n \simeq C(0)\left[\sum_{n=0}^{\infty} \frac{1}{n!} a_n^n (\tilde{\phi}\tau)^n + \frac{1}{\tilde{\phi}} \sum_n \frac{1}{n!} a_{n-1}^n (\tilde{\phi}\tau)^n + \frac{1}{\tilde{\phi}^2} \sum_n \frac{1}{n!} a_{n-1}^n (\tilde{\phi}\tau)^n\right] .$$

If we scale the time variable through $\tau' = \tilde{\phi}\tau$ and if we define

$$F_i \equiv \sum_n \frac{a_{n-i}^n}{n!} (\tilde{\phi}\tau)^n \ , \tag{32}$$

then we may write

$$\frac{C(\tau)}{C(0)} \simeq F_0(\tau') + \frac{1}{\tilde{\phi}} F_1(\tau') + \frac{1}{\tilde{\phi}^2} F_2(\tau') \ . \tag{33}$$

From this we infer

$$D = \int_0^{\infty} C(\tau) d\tau = \frac{5}{4} \tilde{\phi}\left[\int_0^{\infty} F_0(\tau') d\tau' + \frac{1}{\tilde{\phi}} \int_0^{\infty} F_1(\tau') d\tau' + \frac{1}{\tilde{\phi}^2} \int_0^{\infty} F_2(\tau') d\tau'\right] \ . \tag{34}$$

In the above expression (34) we note the following:

1. $F_0(\tau)$ is the highest order contribution in $\tilde{\phi}$, which results from the summation for the convective contribution only. In other words, if we ignore the time dependence of the Hamiltonian, we should get F_0 as the exact velocity correlation function. Therefore, we may say that the correlation $F_0(\tau')$ is the integrable-motion contribution of the

Hamiltonian system, since $\partial_t = 0$ implies the integrability in a 1D Hamiltonian (2D phase space) system. For this reason we suppose that $F_0(\tau')$ represents a zero-integral function and does not contribute to the transport coefficient.

2. The above argument predicts that the diffusion coefficient in the limit $\tilde{\phi} \gg 1$ should scale as $\tilde{\phi}^0$ or, if the integral of F_1 vanishes for some reason, as $\tilde{\phi}^{-1}$. As discussed in Sec. II, the first of these scalings is realizable. However, the correlation function expansion fails to yield the extended-orbit scaling $D \propto \tilde{\phi}^2$, as well as more sophisticated fractional-exponent dependences[6,5] on the amplitude $\tilde{\phi}$. This is due to the limited applicability of the above series approach, since the regrouping and the truncation of terms in an intrinsically asymptotic series is unprovable. Thus the analytic properties of the turbulent diffusivity $D(\tilde{\phi})$ still pose some general questions to be addressed in future studies. Unfortunately, the Kalugin *et al.*[14] approach for steady periodic flows with finite collisional diffusivity $D_{\rm coll}$ is not easily transferrable to our case of time-dependent flow with $D_{\rm coll} = 0$.

B. Simulation

We measure the velocity correlation function for the Hamiltonian (6) through numerical techniques. Since the problem is periodic in phase space with period 2π, we replaced the phase space average by the average over the reduced phase space of $[-\pi, \pi] \times [-\pi, \pi]$. For the measurement of the velocity correlation function, we locate N_p particles randomly in $[-\pi, \pi] \times [-\pi, \pi]$. We integrate the equations of motion of these particles with given initial conditions. During the integration we compute

$$C(\tau) \simeq \frac{1}{N_p} \sum_{i=1}^{N_p} (v_E(0) v_E(\tau)) \tag{35}$$

and take this as an approximation for the velocity correlation function. In this work we take $N_p = 128 \sim 1024$ particles and the integration of the equation of motion was done by

a 5-6 order adaptive Runge-Kutta method (DVERK from IMSL). The truncation error e_T per step was set between 10^{-4} and 10^{-6} and the effect of integration error was controlled by varying e_T so as not to result in erroneous values of $C(\tau)$. In Fig. 6 we show the effect of the finite number of test particles, which can be regarded as the effect of the Monte-Carlo (MC) simulation. For this case we have $\tilde{\phi} = 3$, $e_T = 10^{-4}$, $N_p = 1024$, and 5 different runs are superimposed. We note that although there is a finite difference for the runs, the error seems to be small and the structure of the velocity correlation functions is obviously not affected. We also see that the correlation function decays to zero while oscillating from the maximum at $\tau = 0$. This is a general structure of the computed correlation functions, and it is physically appealing. Also note that the velocity correlation function is normalized to its $\tau = 0$ value. The $C_{\rm MC}(0)/C(0)$ is 1.025 showing an error of few percent compared with the exact 1.

In Fig. 7 we show the velocity correlation function for the $\tilde{\phi} \ll 1$ limit. In Fig. 7(a), $\tilde{\phi} = 0.01,\ 0.02$, and 0.03. The plot shows a steady oscillation. As $\tilde{\phi}$ becomes smaller, the correlation is more nearly periodic in agreement with Eq. (28) in Sec. III. Also we note that the oscillating time scale is the same for $\tilde{\phi} = 0.01,\ 0.02$, and 0.03 and the period of the oscillation is estimated to be 3.1 agreeing with the period π of the driving Hamiltonian. To obtain diffusion in this small amplitude regime there must be a finite decay rate of the two-time velocity correlation function. In the linear limit $\tilde{\phi} \to 0$, this does not occur and the time integral of $C(\tau)$ oscillates without converging. At finite $\tilde{\phi} \to 0$, there is a slow, finite decay rate as shown in Fig. 7(a). For a weak power low decay $t^{-\delta}$ ($\delta > 0$), the value of the time-integral of the correlation function is independent of δ and the correlation time may be defined as the period of the Hamiltonian.

The decay of the velocity correlation function may be also caused by a small intrinsic diffusion $D_{\rm coll}$ due either to collisions or small scale turbulence. We now add the effect of $D_{\rm coll}$ giving small random kicks to δx, δy each time step Δt. The resulting decay of the

two-time correlation function is shown in Fig. 7(b) and the time integral converges giving $D \simeq \tilde{\phi}^2$ for small $\tilde{\phi}$.

In Fig. 8, we plot $C(\tau)/C(0)$ as a function of the non-scaled time τ and the scaled time $\tau' \equiv \tilde{\phi}\tau$ for different $\tilde{\phi}$. From Fig. 8(a) we can guess that the correlations may resemble each other if we rescale the abscissa. That is, if we compress or stretch one of the curves, the correlation may show similar behavior. The result of scaling by $\tilde{\phi}$ is shown in Fig. 8(b), where we may say that the velocity correlation function contains a dominant contribution which does not depend on $\tilde{\phi}$ when regarded as a function of τ'. Therefore we suggest that the correlation function may be written as

$$C(\tau)/C(0) \simeq F_0(\tau') + \mathcal{O}(\tilde{\phi}^{-1}) , \tag{36}$$

where $F_0(\tau')$ is independent of $\tilde{\phi}$ when $\tilde{\phi} \gg 1$. The possibility of this self-similar scaling is anticipated from the power series expression (29) of the velocity correlation function.

VI. Conclusions

We present a scaling theory of the stochastic diffusion in spatially-periodic drift Hamiltonians. We show the possibility of two distinct diffusion scalings in the high-amplitude limit $\tilde{\phi} \gg 1$: $D \propto \tilde{\phi}^2$ in the presence of open isopotentials and $D \propto \tilde{\phi}^0$ if all isopotentials are closed. In the subclass of space-periodic models, the both possiblities are generic. This theory reveals the differences in the geometry of particle orbits between the previously-studied models and predicts both the turbulent diffusion and the Kolmogorov entropy scalings in a qualitative accordance with the existing numerical results.

We also discuss, and numerically test, an alternative approach to studying the stochastic diffusion by computing the particle Lagrangian velocity correlation function. We develop a scaling theory of this correlation function that predicts the saturating diffusion behavior $D \propto \tilde{\phi}^0$, a scaling realizable for Hamiltonians with closed isopotentials. To generalize this

approach and incorporate other diffusion scalings, further work is needed.

We compute the diffusion and the Kolmogorov entropy in a quasi-periodic six-wave Hamiltonian that is designed to cheaply model the random potential of real plasma turbulence. We find the diffusion scaling $D \propto \tilde{\phi}^{0.92\pm0.04}$, which is appreciably steeper than the percolation-theory prediction $D \propto \tilde{\phi}^{0.7}$. This descrepancy is ascribed to the presense of long-range space correlations in the six-wave Hamiltonian $H(x, y, t)$, which definitely does not belong to the universality class of the random-percolation model.[10] In fact, the spatial correlations in the six-wave Hamiltonian are similar to those of quasicrystals that are known to exhibit many properties of perfectly ordered media.[15]

On the contrary, the Kolmogorov entropy is found to scale as $K \propto \tilde{\phi}^{0.56\pm0.17}$ — that is, in a good agreement with the theory.[5] This is well understood as the theoretical derivation of the scaling (15) is not built, unlike that of diffusion, on the knowledge of the uncorrelated-percolation-theory exponents.

Acknowledgements

This work was partially supported by the U.S. Department of Energy and by the NSF-KOSEF Grant for International Collaboration Research.

References

1. W. Horton, Plasma Phys. **23**, 1107 (1981).

2. R.G. Kleva and J.F. Drake, Phys. Fluids **27**, 1686 (1984).

3. W. Horton, Plasma Phys. **27**, 937 (1985).

4. A.A. Chernikov, A.I. Neishtadt, A.V. Rogalsky, and V.Z. Yakhnin, Chaos **1**, 206 (1991).

5. A.V. Gruzinov, M.B. Isichenko, and J. Kalda, Zh. Eksp. Teor. Fiz. **97**, 476 (1990) [Sov. Phys. JETP **70**, 263 (1990)].

6. M.B. Isichenko and W. Horton, Comments Plasma Phys. Controled Fusion **14**, 249 (1991).

7. J. Nycander and M.B. Isichenko, Phys. Fluids **B2**, 2042 (1990).

8. A.A. Vedenov, E.P. Velikhov, and R.Z. Sagdeev, Nucl. Fusion **1**, 82 (1961).

9. J.R. Cary, D.F. Escande, and J.L. Tennison, Phys. Rev. **A34**, 4256 (1986).

10. M.B. Isichenko, "Percolation, statistical topography, and transport in random media," Rev. Mod. Phys., to be published.

11. M.B. Isichenko, J. Kalda, E.B. Tatarinova, O.V. Telkovskaya, and V.V. Yankov, Zh. Eksp. Teor. Fiz. **96**, 913 (1989) [Sov. Phys. JETP **69**, 517 (1989)].

12. M. Ottaviani, "Scaling laws of test particle transport in two-dimensional turbulence," JET Preprint (Abingdon, UK), submitted to Europhys. Lett.

13. G.I. Taylor, Proc. Lond. Math. Soc., Ser. 2, **20**, 196 (1921).

14. P.A. Kalugin, A.V. Sokol, and E.B. Tatarinova, Europhys. Lett. **13**, 417 (1991).

15. P.A. Kalugin, A.Yu. Kitaev, and L.S. Levitov, "$Al_{0.86}Mn_{0.14}$: A six-dimensional crystal," Pis'ma v Zh. Eksp. Teor. Fiz. **41**, 119 (1985) [JETP Lett. **41**, 148 (1985)].

Figure captions

1. The phase portraits of four periodic Hamiltonians: (a) Horton Hamiltonian; (b) Kleva-Drake Hamiltonian with $k = 1$; (c) Kleva-Drake Hamiltonian with $k = 2$; (d) Chernikov *et al.* Hamiltonian.

2. The exponentiation of a liquid curve (the dashed line is the initial position and the solid heavy line is its final position) in a periodically changing shear flow during the first half period (a) and during the second half period (b). The flow corresponds to the Kleva-Drake ($k = 1$) Hamiltonian with the cells of closed streamlines not shown for simplicity. Compared to Fig. 1(b), the pattern is tilted by 45^0.

3. The contour plots of the six-wave Hamiltonian (16) at several moments of time. The area $H(x, y, t) < 0$ is hatched.

4. The dependence of $D(\tilde{\phi})$ (shown by error bars; $N_p = 1024$) and $K(\tilde{\phi})$ (shown by broken line; $N_p = 100$) in a six-wave potential.

5. Time dependence of the interparticle distance for one hundred pairs at $\tilde{\phi} = 10$ in linear (a) and logarithmic (b) scale. The slope K of the least-square fit of $\log d_{12}(t)$ versus t is plotted in Fig. 4.

6. Superposition of 5 different runs for the Lagrangian correlation function in the Horton Hamiltonian with the same parameters to show the effect of numerical simulation for parameters $\tilde{\phi} = 3$, $e_T = 10^{-4}$, $N_p = 1024$.

7. Measured correlation for $\tilde{\phi} = 0.01$, 0.02, and 0.03. Here $N_p = 1024$ and $e_T = 10^{-4}$. (a) Pure Hamiltonian flow; (b) Hamiltonian flow with small background diffusion from $D_{\text{coll}} = \langle \delta x^2 \rangle / (2\Delta t)$.

8. The correlation function $C(\tau)/C(0)$ as a function of τ (a) and as a function of $\tau' \equiv \tilde{\phi}\tau$ (b), showing that $C(\tau)/C(0) \simeq F_0(\tau') + \mathcal{O}(\tilde{\phi}^{-1})$ for $\tilde{\phi} = 20$ and 30.

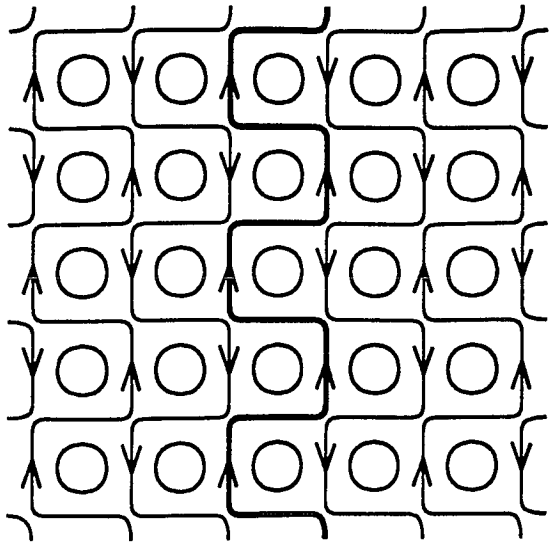

(a)

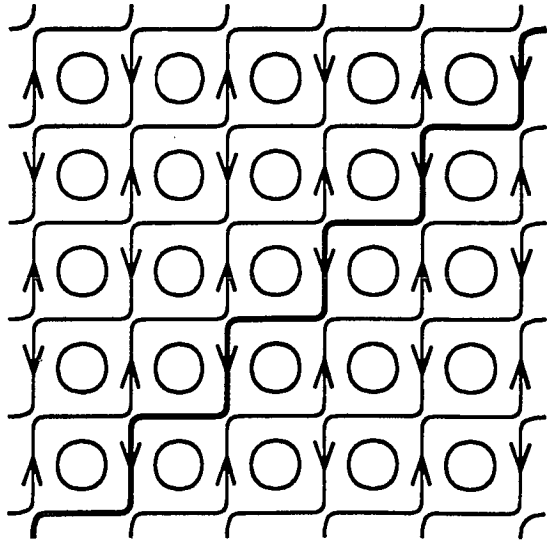

(b)

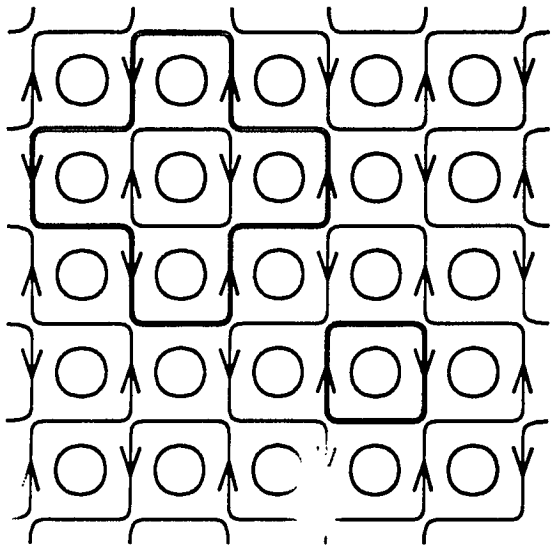

(c)

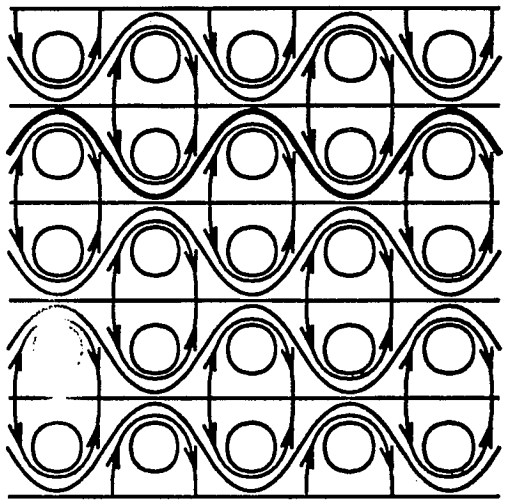

(d)

Fig. 1

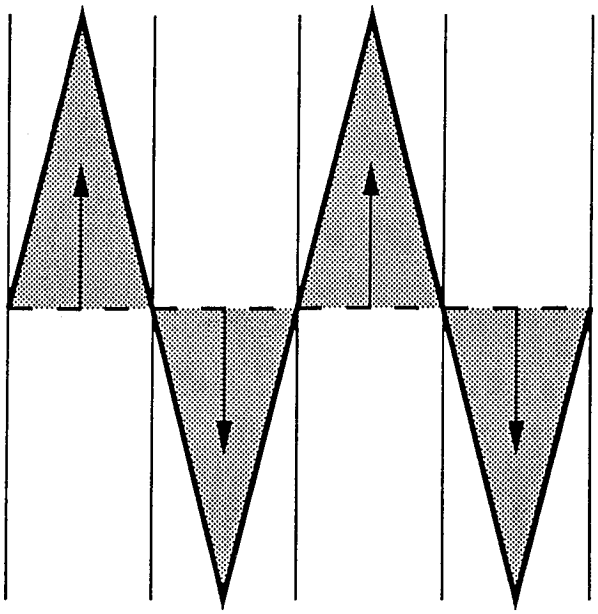

(a)

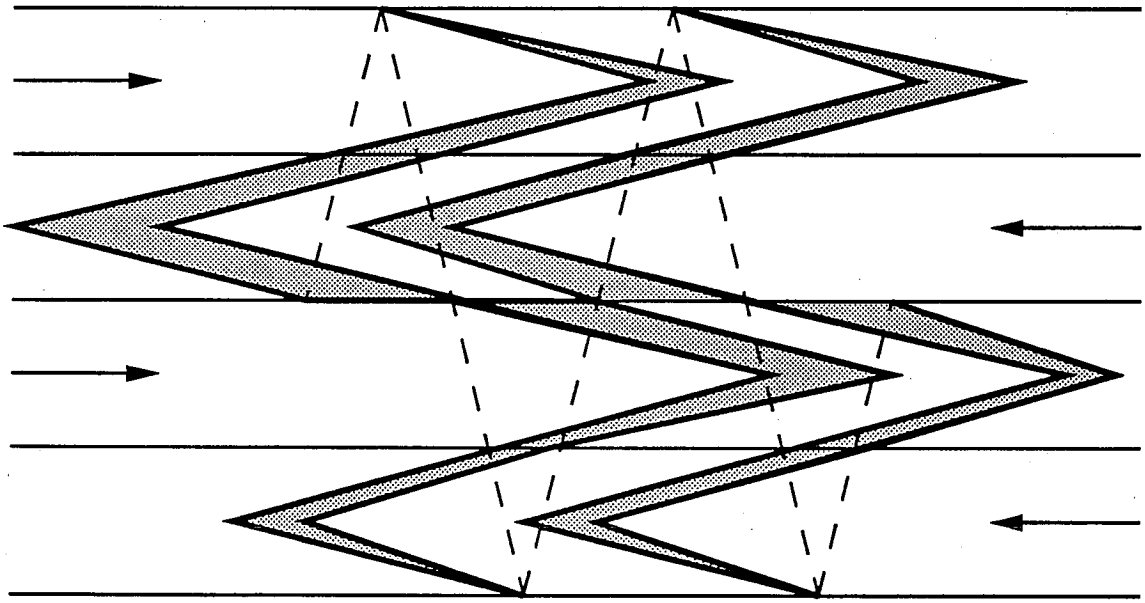

(b)

Fig. 2

t = 0.

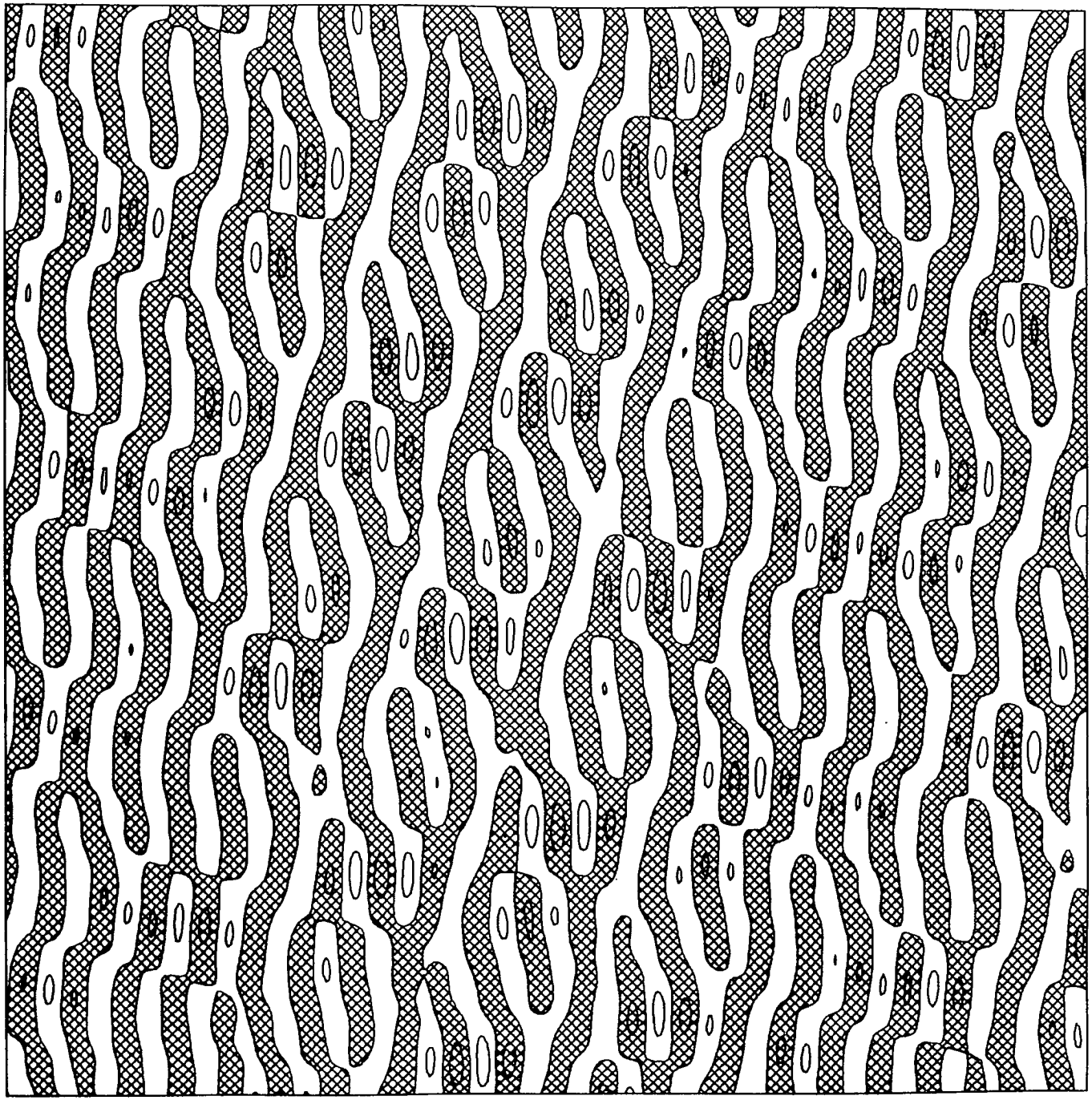

Fig. 3(a)

t = 10.

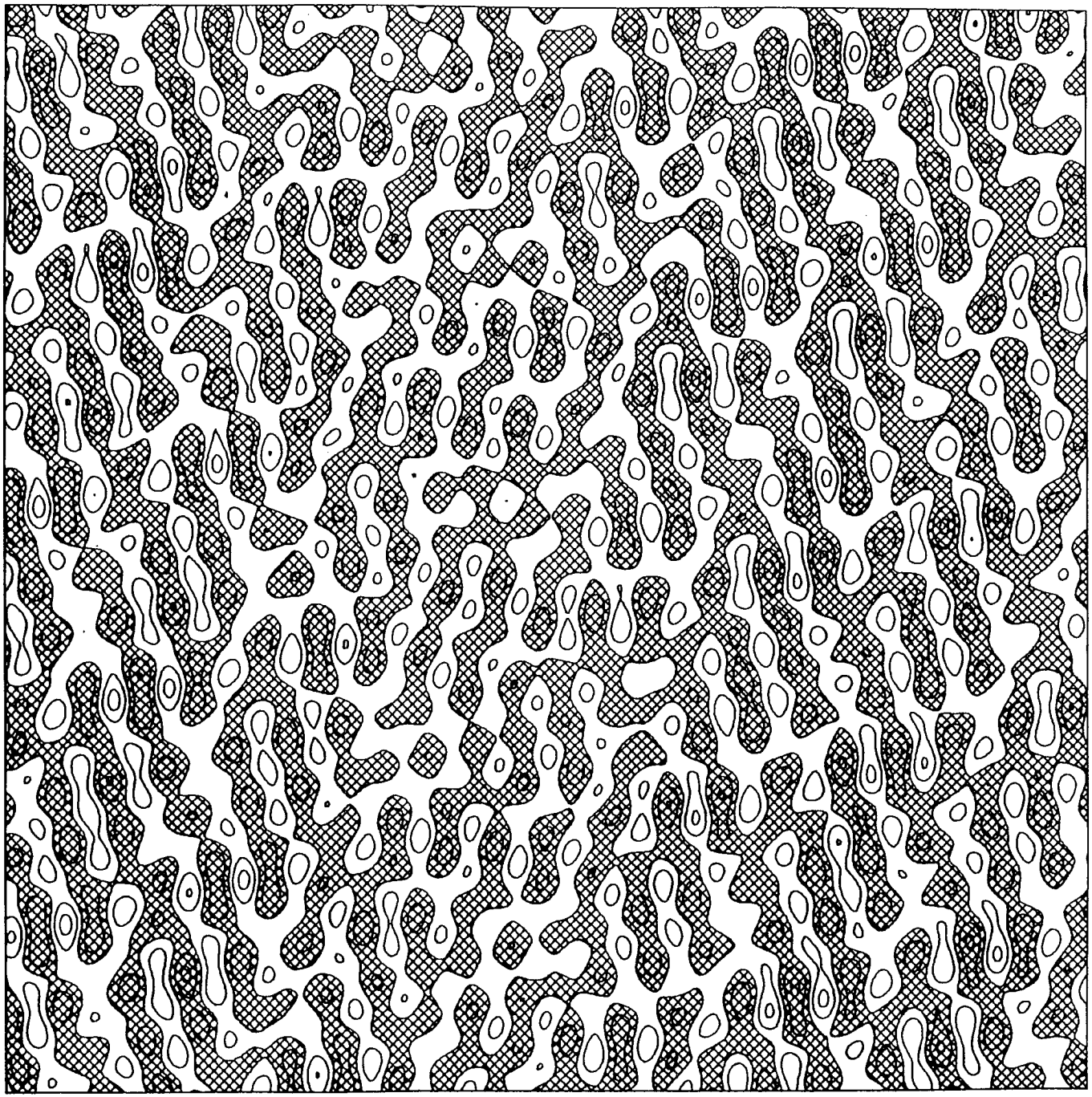

Fig.3 (b)

t = 20.

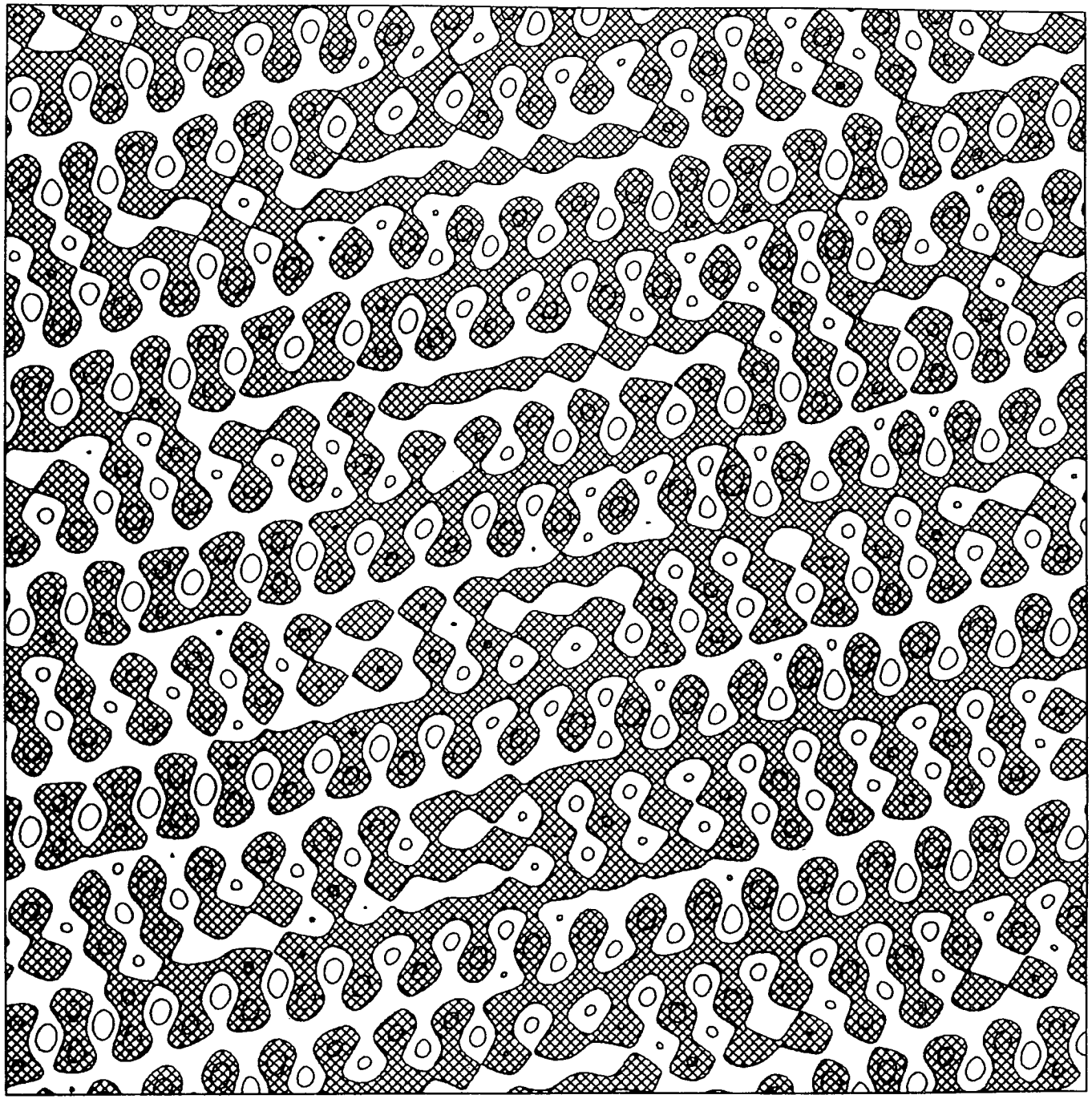

Fig.3 (c)

t = 30.

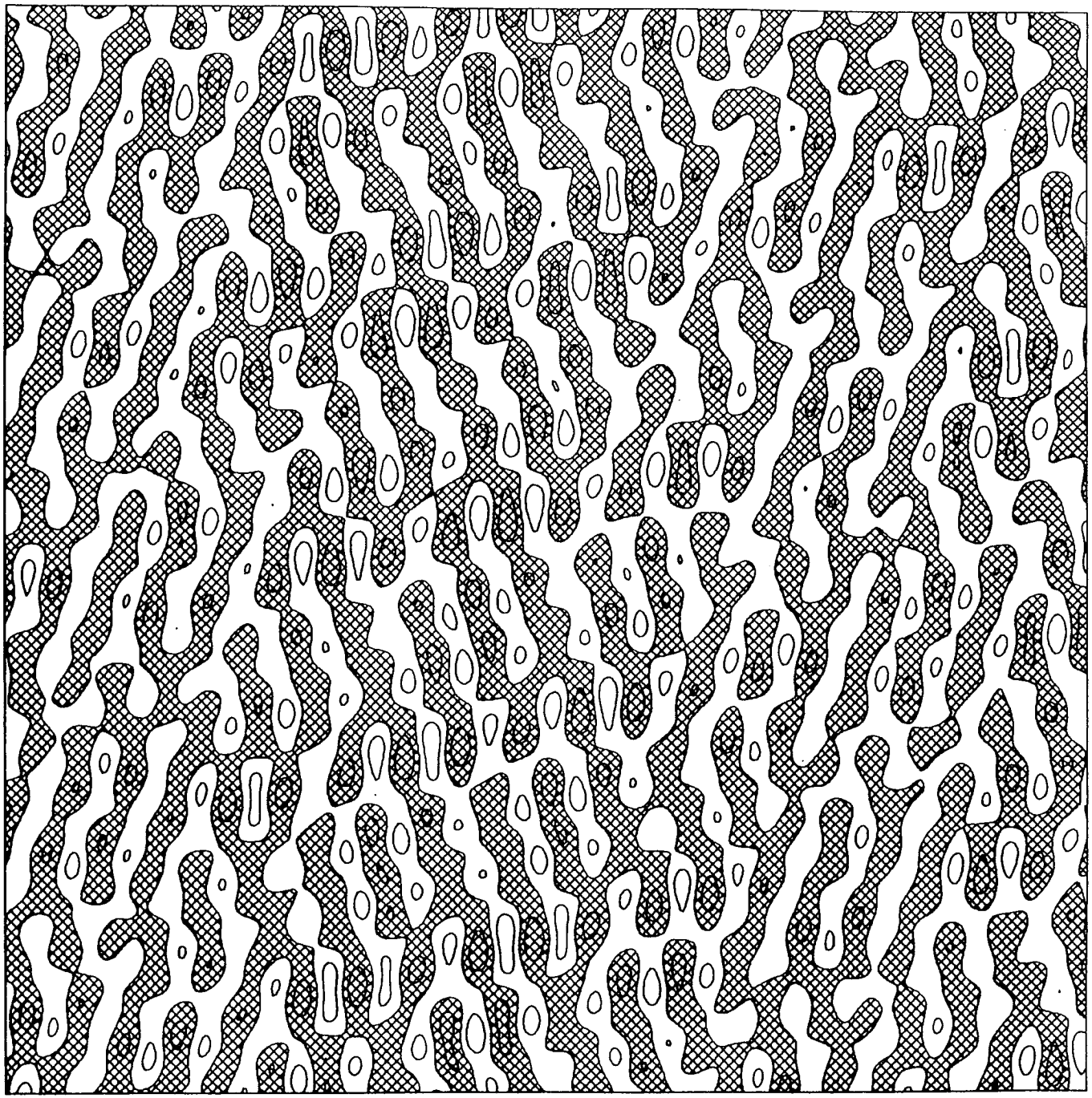

Fig.3 (d)

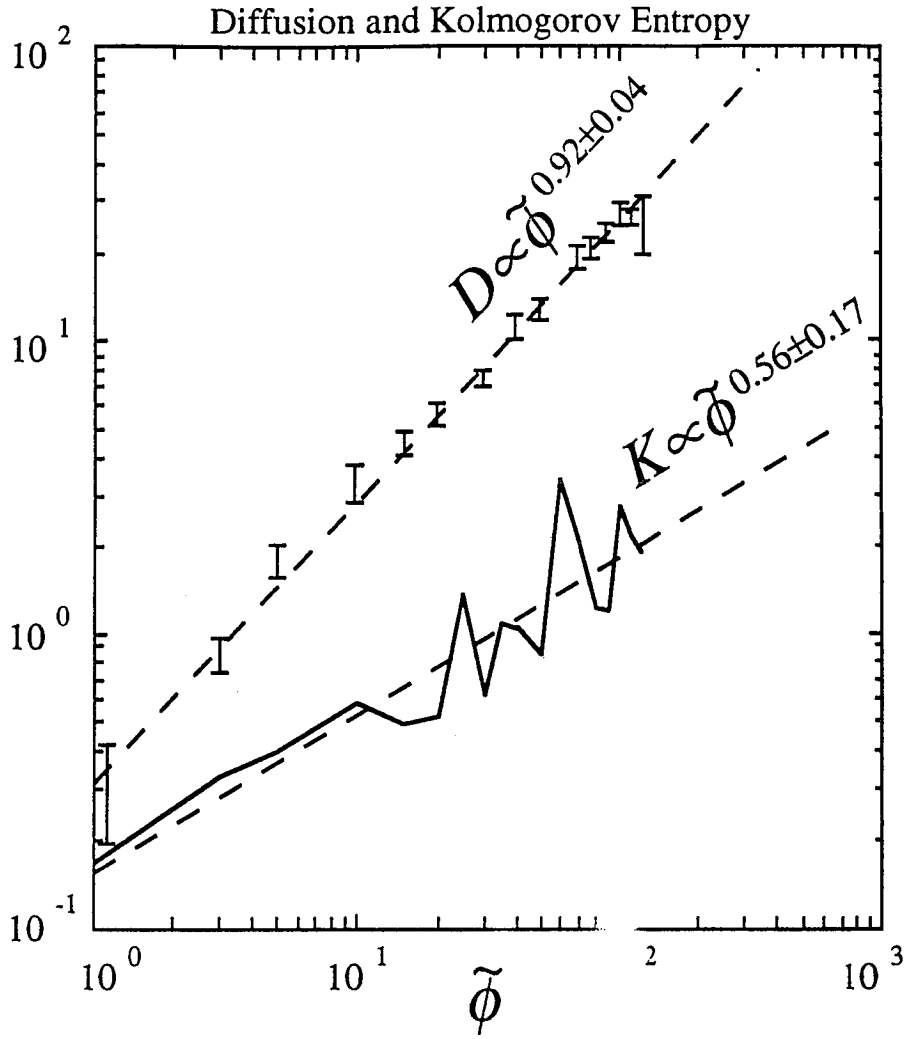
Diffusion and Kolmogorov Entropy
10^2
10^1
10^0
10^{-1}
$D \propto \tilde{\phi}^{0.92\pm0.04}$
$K \propto \tilde{\phi}^{0.56\pm0.17}$
10^0
10^1
2
10^3
$\tilde{\phi}$

Fig. 4

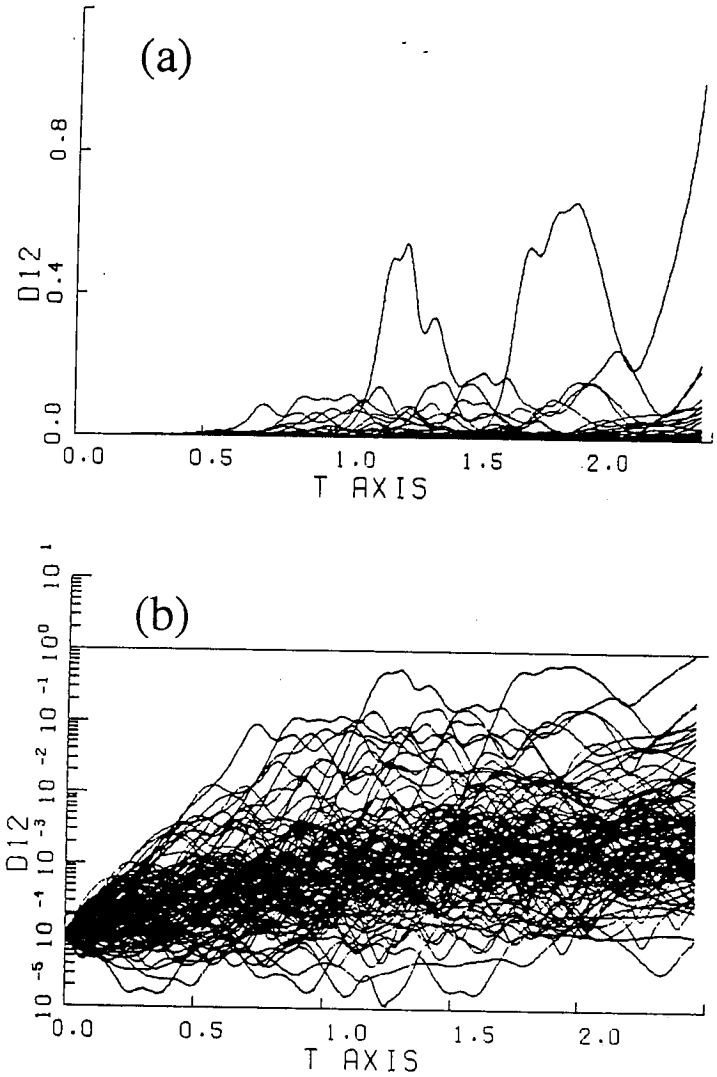
(a)
D12
0.0
0.4
0.8
0.0
0.5
1.0
1.5
2.0
T AXIS
(b)
D12
10^{-5} 10^{-4} 10^{-3} 10^{-2} 10^{-1} 10^{0} 10^{1}
0.0
0.5
1.0
1.5
2.0
T AXIS

Fig. 5

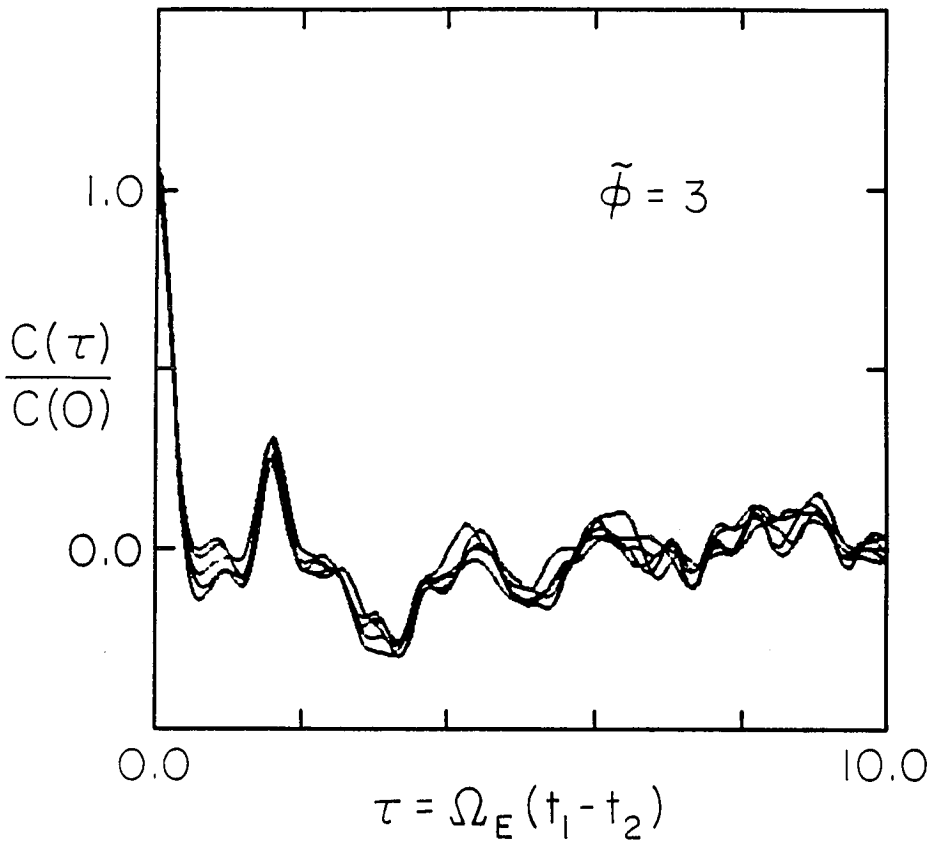

Fig. 6

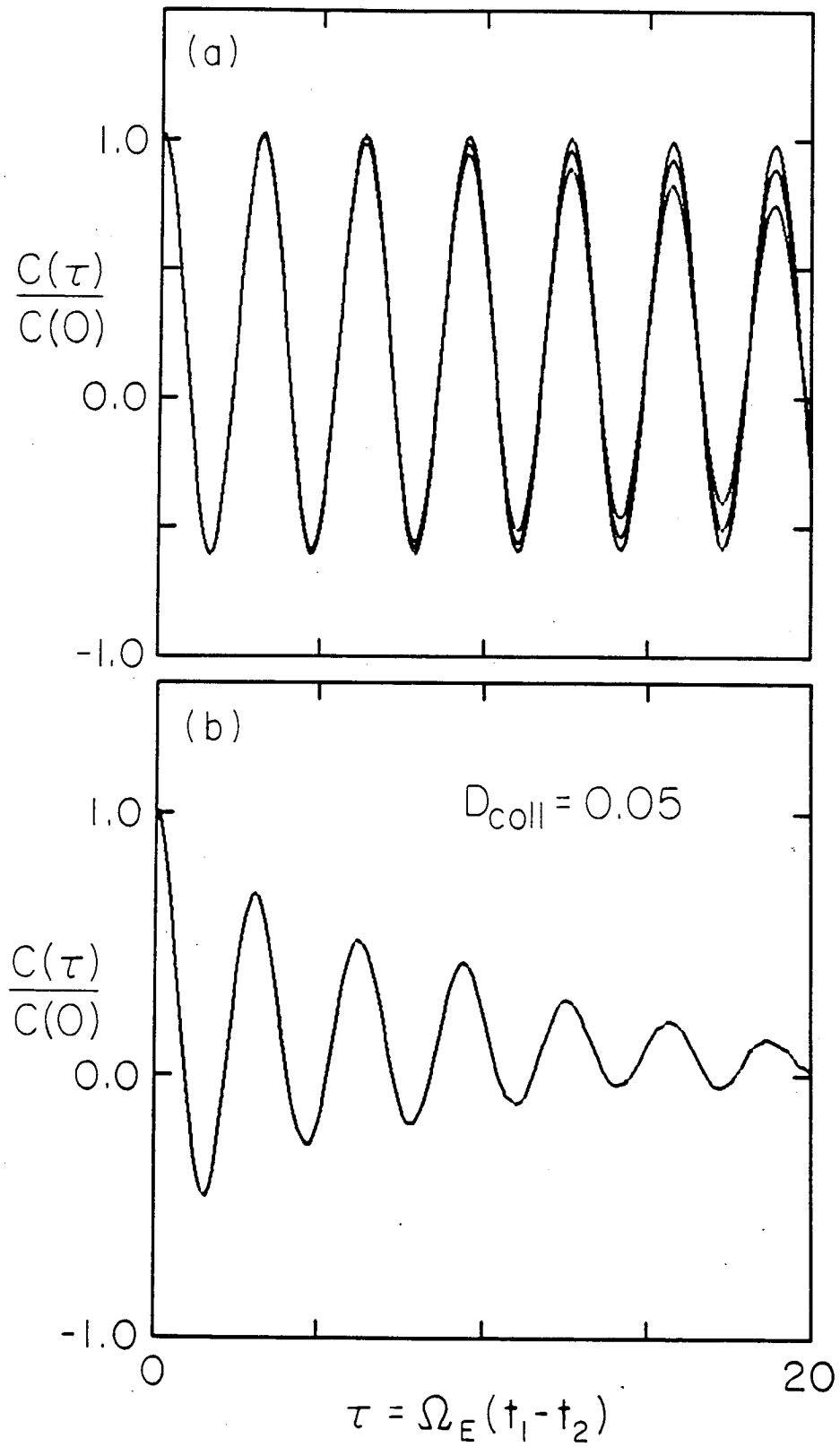

Fig. 7

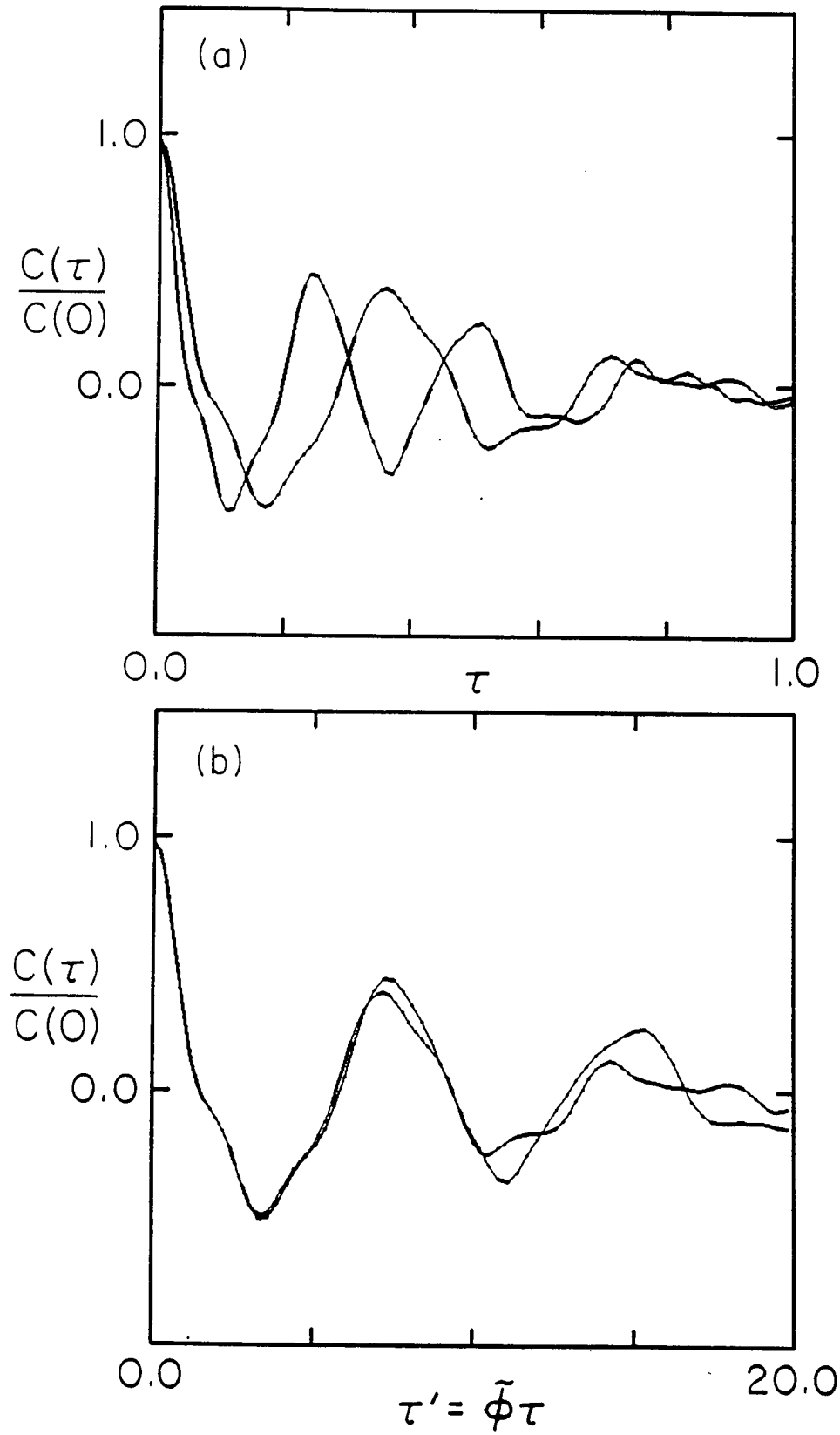

Fig. 8